Journal of Undergraduate Chemistry Research, **2023**, 22(3), 72

THE EFFECT OF ORGANIC SOLVENT POLARITY ON EFFICIENCY OF FLUORESCENCE RESONANCE ENERGY TRANSFER FROM AGGREGATION-INDUCED EMISSION OF THE BIOAIEGEN RIBOFLAVIN TO RHODAMINE B

Chloe Bankhead,* Alex Bean,* Stanley Finlayson,* Matthew Heitmann,* Garret Kuchan,* Madelyn Letendre,* Hayden MacDonald,* Rene Moreno,* Caleb Shin* and Barry W. Hicks †

Department of Chemistry, United States Air Force Academy, USAFA, CO 80840

Abstract

Aggregation-induced emission of BioAIEgens is gaining attention for biological sensing applications due to the large amounts of source materials, ease of production, biocompatibility, and reduced toxicity of BioAIEgens relative to synthetically produced AIEgens. To date, most work on BioAIEgens has been with single emitting species. One recently described BioAIEgen is riboflavin, which forms brightly fluorescent nanoparticles when acidic solutions are diluted into organic solvents. Here we report the preparation of mixed nanoparticles containing riboflavin and rhodamine B that show dual emission by FRET. The effect of nine different solvents (methanol, ethanol, 1-propanol, 1-butanol, isoamyl alcohol, 1-octanol, ethylene glycol, dimethyl sulfoxide and acetonitrile) was examined for effects upon FRET efficiency from donor riboflavin nanoparticles to the red emitting acceptor rhodamine B. The immiscible solvent, 1-octanol, showed the highest FRET efficiency. Although differences were documented in the photophysical properties of monomeric riboflavin, riboflavin AIE nanoparticles and mixed riboflavin/rhodamine B nanoparticles, no specific correlations between solvent polarity or H-bonding capacity was identified.

†Corresponding author: barry.hicks@afacademy.af.edu * Undergraduate researchers and co-authors
Keywords: Riboflavin, aggregation-induced emission, FRET, organic solvents, rhodamine B
Received: July 5, 2023 Accpeted: July 24, 2023 Published: August 19, 2023

Introduction

Aggregation induced emission (AIE) and aggregation caused quenching (ACQ) are properties of materials that lead either to enhanced or decreased fluorescence upon aggregation, respectively (1). Molecules that lead to AIE are termed AIEgens, and natural molecules that demonstrate AIE are called BioAIEgens (2). Vitamin B2, riboflavin (Rf), is a BioAIEgen. In neutral aqueous solutions, Rf fluoresces with a quantum yield (QY) of about 0.26, but that value drops below 10^{-5} when Rf is protonated (HRf^+) in acidic aqueous solutions below pH 1 (3). However, HRf^+ fluorescence can be recovered and enhanced by production nanoparticle aggregates by diluting the acidic aqueous solution into organic solvents (4). AIEgens have numerous applications in sensing (5-9), and BioAIEgens have the added advantages of being more readily available, biocompatible, biodegradable, and less toxic than many of their synthetic counterparts (2,4,10,11).

Most AIE work has been done with a single fluorescent species. However, the ability to tune AIE emission to new wavelengths by FRET has also been demonstrated (12,13). AIE with FRET provides new material optical properties, and thus opens the door to new applications (14,15). However, very little work has been done inducing FRET from BioAIEgens (16,17).

In this work we tested the effects of nine organic solvents, methanol (MeOH), ethanol (EtOH), propanol (PrOH), 1-butanol (BuOH), isoamyl alcohol (IsoAmOH), 1-octanol (OctOH), ethylene glycol (EG), acetonitrile (AcCN), and dimethyl sulfoxide (DMSO) for their ability to enhance FRET efficiency from HRf^+ to rhodamine B ($HRhdB^+$) (Scheme 1) in AIE nanoparticles. $HRhdB^+$ is a unique fluorophore that exists in equilibrium between an open, fluorescent carboxylic acid form and a closed, non-fluorescent lactone form (18). AIE from $HRhdB^+$ alone has also been demonstrated (19,20), and there are many potential applications (21). However, this is the first report of a BioAIEgen used as a FRET donor to the $HRhdB^+$ acceptor.

Material & Methods

Materials

Riboflavin (R9504), rhodamine B (R6626) and all solvents (MeOH, EtOH, PrOH, BuOH, IsoAmOH, OctOH, DMSO, AcCN & ethylene glycol (EG)) were purchased from Sigma Aldrich. Sulfuric acid (A300SI-212) was purchased from Fischer Scientific. Microwell plates (black with flat bottoms for fluorescence, 665096) were from Greiner. All samples were analyzed as 365 μL aliquots in 96-well plates. Since the main construction of the 96-well plates is polystyrene, only organic solvents compatible with polystyrene were analyzed.

Fluorescence Spectra

A Rf stock solution was prepared at 5.0 mM in DMSO; this is the only solvent that can dissolve the neutral form of Rf above 1 mM. This stock solution was diluted to working solutions of 100 μM in each of the 9 organic solvents (thus the working solutions contain 2% DMSO). For spectral analysis of Rf, the working solutions were further diluted to 5.0 μM in each of the solvents (the final DMSO concentration never exceeded 0.1%, except when testing DMSO itself). Then, 365 μL aliquots of each sample were

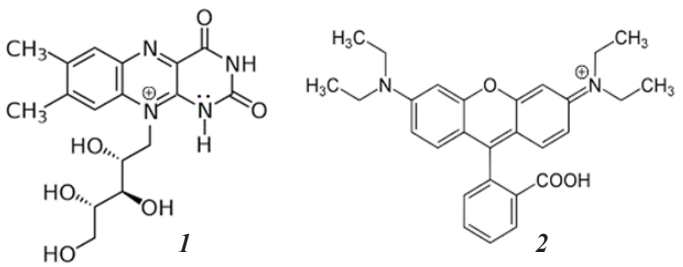

Scheme 1. Structures of the protonated forms of riboflavin (1) and rhodamine B (2) used for AIE and AIE FRET nanoparticle formation.

added to wells in a 96-well plate and analyzed using a Biotech Synergy H4 Microplate Reader. Generally, gain was left at the default setting and the emission slit width varied until the solvent with the highest QY was near maximum, then data was collected for all 9 solvents. All data was analyzed and plotted using Microsoft Excel. For quantum yield comparisons in various solvents, Rf in water was used as the standard with a value of 0.26 (3).

Aggregation-Induced Emission

Methods used were modified from (4). Briefly, stock solutions of HRf^+ were prepared at 200 µM in 1.0 M H_2SO_4 (approximately pH 0). Samples for AIE versus solvent were prepared as seven 1.0-mL samples in 1.5 mL centrifuge tubes. Each sample contained 100 µL of 200 µM HRf^+ (final concentration 20 µM); the 0% sample was diluted with 900 µL of 0.1 M H_2SO_4. The solvent samples contained 20, 40, 60 80 or 90% (v/v) of organic solvent with the remainder being 0.1 M sulfuric acid; thus, all points contained approximately 0.1 M sulfuric acid (pH 1) in the appropriate solvent. Then, 365 µL aliquots were placed into adjacent wells of a 96-well plate and analyzed using a Biotek Synergy H4 Microplate Reader.

Imaging of the samples was done with a GH5 camera. First a normal room light image was captured, then, samples were illuminated with a 450 nm LED light through a yellow long pass filter.

FRET from AIE HRf^+ to $RhdB^+$

FRET efficiency was measured by comparing the acceptor emission versus total emission using equation 1:

$$\text{FRET efficiency} = Fa / (Fa + Fd) \quad (1)$$

where Fa is the integrated intensity of the acceptor emission spectrum and Fd is the integrated intensity of the donor emission spectrum. For the measurements, equal volumes (100 µL) of $HRhdB^+$ and 200 µM HRf^+ (20 µM final), each in 1.0 M H_2SO_4 were mixed with 800 µL of solvent (80%) to induce aggregation of nanoparticles containing both HRf^+ donor and $HRhdB^+$ acceptors. The acceptor concentration was titrated from 5 to 40 µM. Controls containing just HRf^+ or just $HRhdB^+$ (20 µM each) were mixed with an equal volume of 0.1 H_2SO_4. The samples were vortexed and a 365 µL aliquot was removed and analyzed in a Biotech Synergy H4 Microplate Reader. Excitation was at 450 nm and data was collected from 475 to 750 nm. Because the donor and acceptor emission spectra show considerable overlap, the spectra were first deconvoluted in Excel into two Gaussian peaks using Solver. The area of the acceptor was then divided by the total area of both donor and acceptor.

Fluorescence Lifetimes

Fluorescence lifetimes were measured by preparing three samples for each solvent, a monomeric Rf sample, a sample of HRf^+ nanoparticles only, and a FRET sample containing both HRf^+ donor and $HRhdB^+$ acceptor particles. The monomeric sample was prepared by adding 300 µL of a 100 mM stock solution of Rf in 10% DMSO into 2700 mL of the selected solvent to produce 10 µM Rf (final Rf was 10 µM, final DMSO did not exceed 1%). The HRf^+ AIE sample was prepared by adding 150 µL of stock 200 µM Rf solution in 1.0 M sulfuric acid to 150 µL of 0.1 M H_2SO_4 and 2700 µL of selected solvent (final HRf^+ was 10 µM, final solvent 90% v/v). The FRET samples were produced by adding 150 µL of stock 400 µM HRf^+ in 1.0 M H_2SO_4 sulfuric acid to 150 µL of 200 µM $HRhdB^+$ also in 1 M H_2SO_4 and adding 2700 µL of selected solvent (final donor = 10 µM, final acceptor = 20 µM). Each sample was excited with a supercontinuum laser at 450 nm and analyzed for donor emission at 520 nm in an Edinburgh Instruments FLS1000 photoluminescence spectrophotometer. The rate was 9.758 MHz and the data were binned into 1024 channels over 50 ns. Data was analyzed by fitting a single exponential to the log of the decay data which showed minimal χ^2 values.

Results

Figure 1 shows the excitation and emission spectrum of Rf in PrOH. There are two excitation maxima near 350 and 450 nm, and a single emission peak near 525 nm. Other solvents have similar fluorescence spectra, but there are slight differences in the exact maxima (Table 1). HRf^+ nanoparticles likewise have similar spectra (not shown), although exact maxima also vary with solvent. The range in emission maximum varies over 13 nm, from a low of 516 in octanol to a high of 529 in ethylene glycol. There were only slight differences in the position of the 450 nm excitation peak, the range in all 9 solvents being only 5 nm. However, more substantial differences were seen in the position of the excitation peak near 350 nm, with the range occurring over 18 nm. Generally, the small polar alcohols have more red shifted maxima (MeOH & EG) compared to the aprotic solvents (DMSO & AcCN). Likewise, the QY was significantly higher in the aprotic solvents with higher dipole moments than in the alcohols.

All nine solvents led to AIE from HRf^+ (Fig. 2A). Figure 2B is a representative data set from DMSO that shows HRf^+ AIE increases through 90% solvent. Very little AIE is observed below 40% of any organic solvent (Fig. 2C), and, perhaps, even some ACQ is seen for some solvents (MeOH & OctOH). Very little AIE is observed below 40% of any organic solvent, and, perhaps, even some ACQ is seen for some solvents (MeOH & OctOH). Working with the immiscible solvents was complicated by the fact that they partition into two layers. To include a portion of both layers,

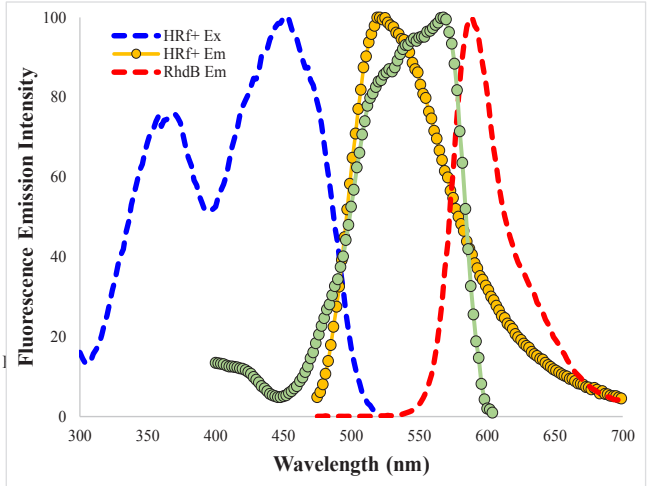

Figure 1. The normalized excitation (blue dotted line) and emission (gold circles) of monomeric Rf, along with the excitation (green circles) and emission (dotted red line) of HRhdB+. The extensive overlap between Rf emission and HRhdB+ excitation indicates that the two should make a good FRET pair, and it has an absorbance minimum at 450 nm near the Rf maximum. There are moderate differences in the Rf and HRhdB+ maxima in other solvents (Table 1), all spectra of monomeric Rf were similar regardless of solvent.

samples were vortexed immediately before removing an aliquot for testing. Additionally, there is a change in QY from HRf^+ AIE nanoparticles compared to those of monomeric Rf; in contrast to the values seen in Table 1, the solvents with the most intense emission are the smaller alcohols. Also, both OctOH and AcCN had relatively low emissions. The solvent percentages to reach half maximal value of AIE are largely in the 40-50 range (Table 2). There is also a general trend of increasing amount of solvent required to reach half maximal emission for the alcohols with increasing carbon number.

AIE nanoparticles can undergo FRET with HRf^+ as the donor and $HRhdB^+$ as the acceptor. $HRhdB^+$ alone also exhibits AIE in MeOH (Fig. 3A) and can act as an acceptor for FRET. As the concentration of acceptor increases the emission from the donor only shows a corresponding decrease in intensity suggestive of FRET. Interestingly, $HRhdB^+$ can also show AIE in MeOH (Fig. 3A), but in other solvents $HRhdB^+$ showed minor ACQ. This unusual behavior complicates the use of static emission spectra as definitive evidence of FRET, even when donor emission decreases with increasing acceptor, since the acceptor emission does not show a similar increase. This was done by varying the concentra-

Table 1. Fluorescence parameters of Rf in various organic solvents

Solvent	*Dipole Moment (D)*[1]	*Dielectric Constant*	*λ of Max Excitation (nm)*	*λ of Max Emission (nm)*	*QY*
MeOH	1.68	33	368, 447	528	0.28
EtOH	1.69	16.2	354, 448	519	0.50
PrOH	1.56	2.2	364, 447	522	0.58
BuOH[2]	1.66	17.8	358, 449	523	0.25
IsoAmOH[2]	1.70	14.7	355, 448	519	0.33
OctOH[2]	1.76	10.3	357, 452	516	0.15
Et Glycol	2.27	37.0	368, 452	529	0.20
DMSO	3.96	46.7	350, 453	523	0.72
AcCN	3.93	37.5	355, 442	518	0.62

1. Literature values.
2. These solvents are not miscible with water/aqueous sulfuric acid.

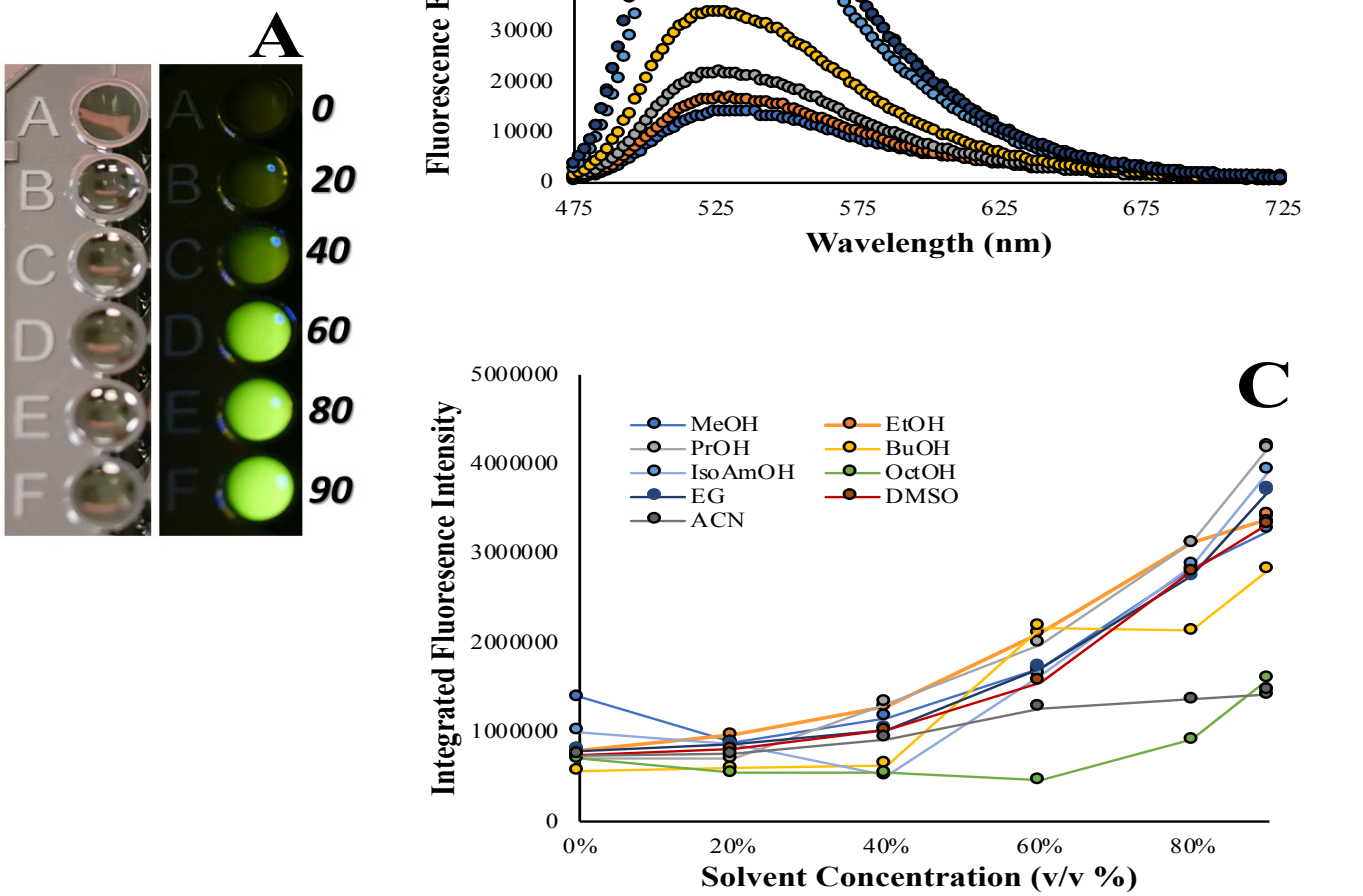

Figure 2. Riboflavin AIE. A. mages of HRf^+ AIE in a microwell plate used for quantitative measurements clearly demonstrates the increase in emission of HRf+ with increasing organic solvent. B. Riboflavin (20 μM) was excited at 450 nm after AIE in different concentrations of DMSO (0-90% v/v). Emission from HRf^+ nanoparticles increases as the organic solvent concentration increases. Duplicates at 90% are provided as a measure of repeatability/reliability of data sets. C. Data for HRf^+ AIE from all 9 solvents; all solvents displayed AIE. Emission spectra areas under the curve were obtained after excitation at 450 nm for the HRf^+ nanoparticles at each concentration in each of the 9 solvents. In contrast to the QY of monomeric neutral Rf, for AIE, PrOH and MeOH have the highest intensities whereas OctOH and AcCN nitrile have the lowest.

tion of RhdB$^+$ to cause emission through FRET. From Fig. 3B, as the concentration of RhdB increased and the concentration of acid decreased, the emission from RhdB$^+$ increased. The lowest FRET efficiency was 0.37 in the lowest concentration of PrOH and the highest efficiency was 0.87 in the highest concentration of OctOH. All of the slopes were similar across the solvents and were all positive, indicating increased FRET as the concentration of HRhdB$^+$ increased. The values of the slopes were EG:0.0035; MeOH:0.0093; EtOH:0.0045; PrOH:0.0062; BuOH:0.0023; Iso-AmOH: 0.0057; OctOH:0.0102; DMSO:0.0034; AcCN:0.0056.

Table 2. Percent Solvent Required to Achieve Half of Maximum AIE

Solvent	*Percent Solvent (%)*
MeOH	40
EtOH	41
PrOH	49
BuOH[1]	46
IsoAmOH[1]	59
OctOH[1]	45
EG	48
DMSO	45
AcCN	49

1. These solvents are not miscible with water/aqueous sulfuric acid.

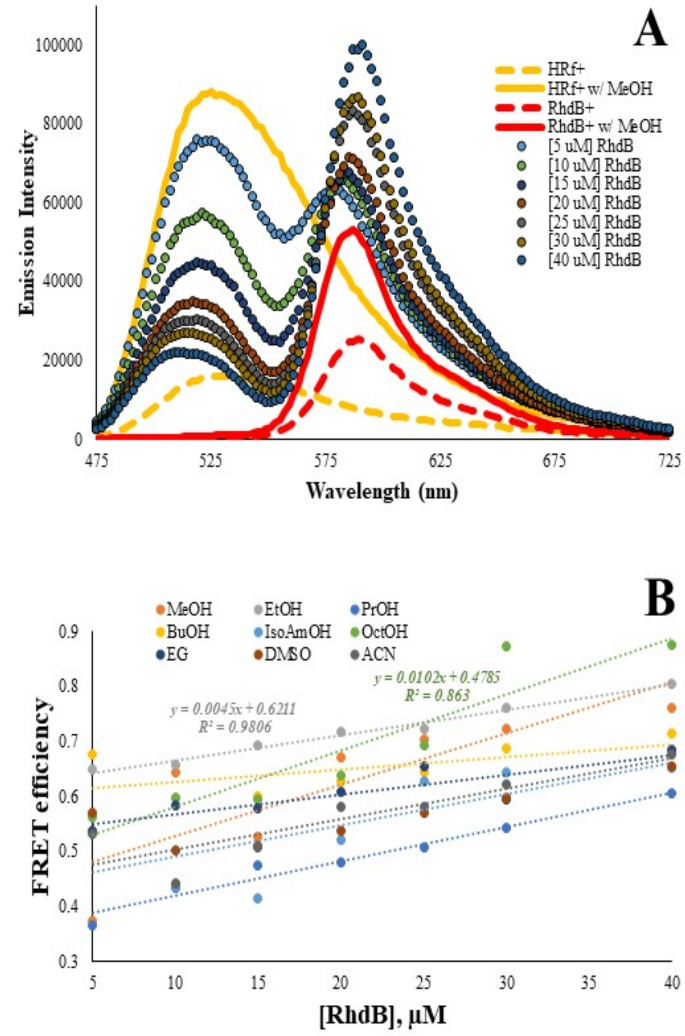

Figure 3 Solvent effects on FRET from HRf$^+$ AIE nanoparticles to HRhdB$^+$. A. Sample data is shown for MeOH. All solvents resulted in AIE from HRf$^+$ (gold solid and dashed lines are with or without solvent, respectively) as well as from HRhdB$^+$ alone (red solid and dashed lines are with or without MeOH, respectively) FRET is indicated by the decrease in absorbance of the HRf$^+$ donor as acceptor concentration increases. B. FRET efficiency versus the HRhdB$^+$ acceptor concentration. As the concentration of RhdB was increased the FRET efficiency also increased to values exceeding 80%. The most efficient solvents were OctOH & EtOH (regression equations and R^2 values indicated), and the least efficient solvent was IsoAmOH.

AIE and FRET were demonstrated unambiguously in all solvents by measuring the lifetimes in the absence and presence of the acceptor. RhdB$^+$ was selected as the acceptor because it has nearly complete spectral overlap with the Rf donor; it is however, complicated by the overlap in emission spectra. For clarity only AcCN lifetime data is shown in Fig. 4; the lifetime values were obtained by fitting single exponentials to the log data. Two observations stand out. First the lifetime of monomeric, neutral Rf is different from that of HRf$^+$ AIE nanoparticles. Second, the lifetimes of nanoparticles containing both donor HRf$^+$ and HRhdB$^+$ are shorter in the presence of acceptor (Table 3). Aggregated HRf$^+$ nanoparticles from AcCN showed the shortest lifetime at 1.28 ns (only 38% of the monomeric lifetime), and those from OctOH had the longest

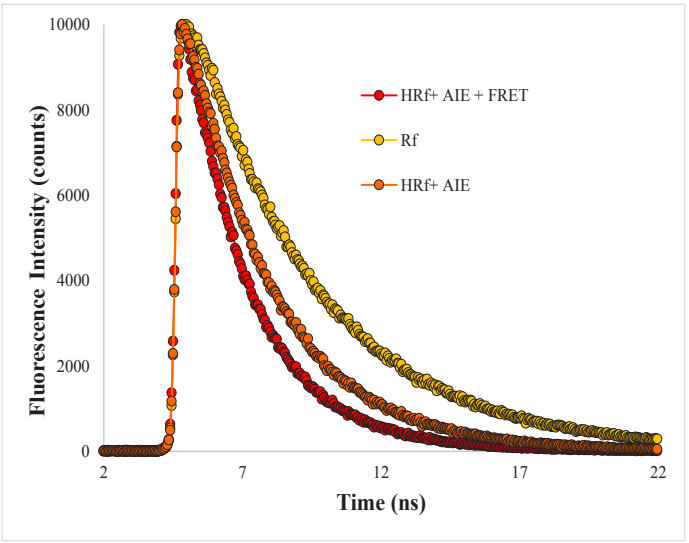

Figure 4: Emission intensity (counts) is plotted against time (nanoseconds) for Rf (yellow circles), and HRf$^+$ in AcCN solvent without (orange circles) and with HRhdB$^+$ (red circles). The AIE nanoparticles have a shorter lifetime than the monomeric Rf in solvent. Furthermore, in the presence of HRhdB$^+$ acceptor, the HRf$^+$ aggregates had a shorter of lifetime indicating that FRET is indeed occurring.

Table.3 Fluorescence lifetimes of Rf, HRf$^+$, and HRf$^+$ with RhdB.

Solvent	*Rf (ns)*	*HRf$^+$ (ns)*	*HRf$^+$ + HRhdB$^+$ (ns)*
MeOH	4.47	2.59	1.85
EtOH	5.23	3.25	3.12
PrOH	4.6	3.15	2.46
BuOH[1]	4.59	3.27	2.70
IsoAmylOH[1]	4.85	4.53	3.97
OctOH[1]	5.11	4.94	4.71
EG	5.16	4.16	3.63
DMSO	2.90	2.80	2.72
AcCN	3.34	1.28	1.00

1. Solvents are not miscible with water / aqueous sulfuric acid.

at 4.94 ns. The shortest lifetime in the presence of $HRhdB^+$ was also from AcCN of only 1.00 ns, and that with the longest lifetime was from OctOH at 4.71 ns. Interestingly, in EtOH, DMSO and OctOH the difference between HRf^+ aggregates in the absence and presence of acceptor was quite modest.

Discussion

Previous work on HRf^+ AIE was done mostly with excitation in the UV at either 365 nm (for visualization and imaging) or at 350 nm for spectroscopy, and that work also relied mostly upon inducing aggregation with tetrahydrofuran (THF) (4). For bioimaging applications of HRf^+ nanoparticles, blue light at 450 nm would be preferable as it is much less phototoxic than UV (22), as would the use of solvents that are less toxic than THF (23), which can aid in proliferation of this technology in medical applications. We show in this work that HRf^+ nanoparticles can be imaged and analyzed when excited at 450 nm and that those aggregates can be produced with less hazardous solvents.

We specifically examined a series of H-donor solvents (alcohols with 1-8 carbons) to examine the effect of decreasing polarity, as well as to examine AIE in immiscible solvents. Differences in Rf and HRf+ excitation spectra, emission spectra and QY were evident in different solvents, however, no clear correlation between solvent polarity (dipole moment or dielectric constant, not shown) was identified. AIE can result from numerous mechanisms including restricted molecular vibration or rotation, restricted access to dark states, twist charge transfer, or excited-state intramolecular proton transfer (ESIPT) (1,4). For HRf^+ ESIPT has been postulated to be the predominate mechanism (4). For monomeric Rf the two solvents with the highest QY were DMSO and AcCN, whereas the solvents that produced the brightest AIE nanoparticles were PrOH and MeOH. Others have shown that solvent polarity affects the probability of electron transitions in Rf from the ground state, S_0, to higher excited states (S_2-S_4) explaining the observed differences in the UV absorbance spectra (24), but why the different solvents produce nanoparticles with nearly 4-fold difference in intensity is not clear. Additionally, the HRf^+ nanoparticles were far more heat stable than monomeric Rf (not shown). The nature of the AIEgen (25), the choice of solvent (26), the mole fraction of water present (27), the counter-ion chosen (28) and even the method of mixing (29) can all play a role in the particle size distribution of nanoparticles, and this likely alters the photochemistry of the HRf^+ nanoparticles produced. However, the lack of significant correlation between photochemical properties of the monomeric AIEgen and the AIE nanoparticles produced from it in various organic solvents suggest predicting *a priori* the best solvent for a given AIEgen may not be possible without a much more extensive dataset.

As with simple AIE, the results from our AIE FRET work indicate that there are no simple correlations between choice of organic solvent and the photochemical properties that result in the most efficient FRET. The two solvents that showed the highest FRET efficiency from HRf^+ to $HRhdB^+$ were OctOH and EtOH, and neither of these were the brightest for monomeric Rf or for HRf^+ nanoparticles. That FRET is occurring is implied in the emission spectra; as acceptor concentration increased the donor emission decreased. This implies that the nanoparticles of donor and acceptor are in close association. Differences in FRET efficiency might very well be due to the type of nanoparticle aggregates formed. FRET was further verified by the decrease in lifetime of the HRf^+ donor in the presence of the $HRhdB^+$ acceptor (30).

We chose $HRhdB^+$ for the acceptor in this work because of its requirement for acidic solutions to be an active fluorophore made it compatible with HRf^+ (31), and because of its near complete spectral overlap with HRf^+. However, this made demonstration of FRET more complex because of the need to do emission peak deconvolution. Examining numerous further red emitting acceptors (Nile Red, Alexa Fluor 647, chlorophyll a, etc.) in the same solvents might also be informative. In particular, Alexa Fluor 647 is an anionic red emitting dye (32), and it might alter the type of nanoparticle produced with the cationic HRf^+ donor, and perhaps in a pH-dependent manner. As with the need to examine a broader set of solvents to gain greater insight into the relationship between solvent structure and AIE emission, a broader set of FRET acceptors likewise needs to be characterized if any correlation is to be found.

Acknowledgements

We would like to thank the US Air Force Academy Chemistry Department and the Chemistry Research Center for funding this research. Google Bard AI was used for some sections of the paper for comparison with those prepared by the authors, which resulted in minor editing of early drafts. All final written versions were the work of the authors, and no portion of this work was written solely by AI.

References

1. Hong Y., Yuning; L.J.W.Y.; Tang, B.Z. *Chem. Soc. Rev.*, **2011**, 40.11, 5361-5388.
2. Lee, M.M.S.; Yu, E.Y.; Chau, J.H.C.; Lam, J.W.Y.; Kwok, R.T.K.; Wang D. *Biomaterials.* **2022**, 288, 121712.
3. Drössler, P.; Holzer, W.; Penzkofer, A.; Hegemann, P. *Chem. Phys*., **2002.** 282.3, 429-439.
4. Xu, L.; Liang X.; Zhang S.; Wang B.; Zhong S.; Wang M. *Dyes and Pigments.* **2020**, 182, 108642.
5. Zhou, H.; Chua, M.H.; Tang, B.Z.; Xu, *J. Poly. Chem*. **2019**, 10.28, 3822-3840.
6. Mise, Y.; Imato, K.; Ogi, T.; Tsunoji, N.; Ooyama, Y. *New J. Chem*. **2021**, 45.9, 4164-4173.
7. Qi, F.; Li, Y.; Wang, L.; Li, C.; Wang, J.; Liu, Y. *Chem. Commun.* **2016**, 52.15, 3123-3126.
8. Hu, J.; Liu, Y.; Zhang, X.; Han, H.; Li, Z.; Han, T. *Dyes and Pigments*. **2021,** 192, 109393.
9. Li, C.; Gao, C.; Lan, J.; You, J.; and Gao, G. *Org & Biomol. Chem*. **2014**, 12.47, 9524-9527.
10. Cai, X.; Lin, Y.; Li, Y.; Chen, X.; Wang, Z.; Zhao, X. *Nature Commun*. **2021**, 12.1, 1773.
11. Heo, J.; Murale, D.P.; Yoon, H.Y.; Arun, V.; Choi, S.; Kim, E. *Aggregate*. **2022**, 3.2, e159.
12. Nhien, P.Q.; Chou, W.; Cuc, T.T.K.; Khang, T.M.; Wu, C.; Thirumalaivasan, N. *ACS Appl. Mat. & Interfaces*. **2020**, 12.9, 10959-10972.
13. Wang, Z.; Fang, Y.; Tao, X.; Wang, Y.; Quan, Y.; Zhang, S. *Polymer.* **2017**, 130, 61-67.
14. Wang, D.; Chen, J.; Ren, L.; Li, Q.; Li, D.; Yu, *J. Inorg. Chem.*

Front. **2017**, 4.3, 468-472.
15. Wu, L.; Huang, C.; Emery, B.P.; Sedgwick, A.C.; Bull, S.D.; He, X. *Chem. Soc. Rev.* **2020,** 49.15, 5110-5139.
16. Sun, J.; He, X. Aggregate. 2022, e282.
17. Wang, S.; Zhou, K.; Lyu, X.; Li, H.; Qiu, Z.; Zhao, Z.; Tang, B.Z. *Chem. & Biomed. Imaging*, **2023**, in press.
18. Stephenson, C.J.; Shimizu, K.D. *Org. & Biomol. Chem*. 2010, 8.5, 1027-1032.
19. Yu, H.X.; Zhi, J.; Chang, Z.F.; Shen, T.; Ding, W.L.; Zhang, X.; Wang, J.L. *Mat. Chem. Front.* **2019**, 3(1), 151-160.
20. Mathivanan, M.; Tharmalingam, B.; Anitha, O.; Thiruppathiraja, T.; Lakshmipathi, S.; Malecki, J.G. *J. Molec. Liquids*. **2023**, 121845.
21. Lee, M.M.S.; Yu, E.Y.; Chau, J.H.C.; Lam, J.W.Y.; Kwok RTK, Wang D, et al. Biomaterials. **2022,** 288, 121845.
22. Kolega, J. *Biochem. Biophy. Res. Commun*. 2004, 320.3, 1020-1025.
23. Joshi, D.R.; Nisha, A. J. Pharm. Res. Int. 2019, 28.3, 1-18.
24. Daidone, I.; Amadei, A.; Aschi, M.; Zanetti-Polzi, L. *Spectrochimica Acta Part A: Molec. Biomolec. Spectro*. **2018,** 192, 451-457.
25. Dineshkumar, S,; Raj, A.; Srivastava, A.; Mukherjee, S.; Pasha, S.S.; Kachwal, V. " *ACS Appl. Mat. & Interfaces*. **2019**, 11.34, 31270-31282.
26. Anand, V.; Mishra, R.; Barot, Y. *Dyes and Pigments*. **2021**, 191, 109390.
27. Das, B.; Dolai, M.; Dhara, A.; Ghosh, A.; Mabhai, S.; Misra, A. J. Phys. Chem. A. 2021, 125.7, 1490-1504.
28. Leduskrasts, K.; Suna, E. *RSC Adv*. **2020**, 10.62, 38107-38113.
29. Wang, M.; Yang, N.; Guo, Z.; Gu, K.; Shao, A.; Zhu, W. *Indus. & Eng. Chem. Res*. **2015**, 54.17, 4683-4688.
30. Biskup, C.; Zimmer, T.; Kelbauskas, L.; Hoffmann, B.; Klocker, N.; Becker, W. *Microscopy Res. & Tech.* **2007**, 70.5, 442-451.
31. Karpiuk, J.; Grabowski, Z.R.; Schryver, F.C.D. *Proc. of the Indian Acad. Sci.-Chem. Sci.* **1992**, 104, 133-142.
32. Li, D. *Development of immunoassay screening methods using long wavelength fluorescence.* PhD. Diss. Loughborough University, Loughborough, England, United Kingdom, 2004.